

A Novel Approach for Effective Dose Measurements in Dual-Energy

by

Brett Joshua Mattison

Graduate Program in Medical Physics
Duke University

Date:_____

Approved:

Terry Yoshizumi, Supervisor

Robert Reiman

James Colsher

Thesis submitted in partial fulfillment of
the requirements for the degree of Master of
Science in the Graduate Program
in Medical Physics of
Duke University

2014

ABSTRACT

A Novel Approach for Effective Dose Measurements in Dual-Energy

by

Brett Joshua Mattison

Graduate Program in Medical Physics
Duke University

Date: _____

Approved: _____

Terry Yoshizumi, Supervisor

Robert Reiman

James Colsher

An abstract of a thesis submitted in partial
fulfillment of the requirements for the degree
of Master of Science in the Graduate
Program in Medical Physics of
Duke University

2014

Copyright by
Brett Joshua Mattison
2014

Abstract

Purpose:

Our goal was to test a novel concept approximating organ dose measurements using the single mean energy of the two sources in dual-energy (DE) CT environment. Therefore, the purpose of this study was two-fold: (1) To obtain experimental validation of dose equivalency between Metal Oxide Silicon Filed Effect Transistor (MOSFET) and ion chamber (as gold standard) under a dual-energy environment; (2) To estimate the effective dose (ED) using MOSFET detectors and an anthropomorphic phantom in DE CT scans.

Materials and Methods:

A Siemens SOMATOM Definition Flash dual source CT (DSCT) DSCT (Siemens Corp., Munich, Germany) was employed for the study. The scanner was operated at 80kVp/140kVp (Sn added) using an abdomen/pelvis scanning protocol. A five-phase approach was used. Specific goals for each phase are as follows: (1) Characterize the mean energy from the combined clinical 80kV/Sn140kV beams; (2) Estimate the f-factor for tissues from the mean energy; (3) Calibrate the MOSFET detectors using the mean energy; (4) Validate MOSFET calibration with a CTDI phantom; (5) Measure organ doses for a typical abdomen/pelvis scan using a male anthropomorphic phantom and derive ED using ICRP 103 tissue weighting factors. For validation of dose equivalency, a

MOSFET detector and ion chamber measured the dose at the center cavity of a CTDI body phantom. A student t-test was used to determine if the difference between the two was statistically significant.

Results:

The mean energy was calculated to be 67 keV based on the corresponding spectra for the clinical DE beams. Using the Mean Energy Method, the tissue dose in the center cavity of the CT body phantom was $2.08 \pm (2.70\%)$ cGy with an ion chamber and $2.20 \pm (4.82\%)$ cGy with MOSFET respectively with a percent difference of 5.91% between the two measurements. The results ($p = 0.15$) showed no statistically significant difference. ED for DE abdomen/pelvis scan was calculated as $5.01 \pm (2.34\%)$ mSv by the MOSFET method and 5.56 mSv by the DLP method respectively.

Conclusion:

There has been no physical method to measure organ doses in DE CT scans. We have developed and validated a novel approach, the *Mean Energy Method - for organ dose estimation* in DE CT scans. ED from the anthropomorphic phantom compared well (within 11%) between the MOSFET method and DLP method.

Contents

Abstract	iv
List of Tables	ix
List of Figures	x
Acknowledgements	xii
Chapter 1. A Novel Approach for Effective Dose Measurements in Dual-Energy	1
1.1 Introduction.....	1
1.1.1 Duel Energy Computed Tomography vs. Conventional Computed Tomography.....	2
1.1.2 Advantages of DSCT.....	2
1.1.3 Difficulties	3
1.1.4 Objective	3
1.2 Materials and Methods.....	4
1.2.1 Characterize the mean energy from the combined clinical 80kVp/140kVp (Sn added) beams.....	5
1.2.2 Estimate the f-factor	8
1.2.3 MOSFET Detector Calibration:.....	9
1.2.4 Calibration validation.....	11
1.2.5 Organ Dose Measurement with DSCT.....	14
1.3 Results	15
1.4 Conclusion.....	18
1.5 Discussion.....	18

1.6 Future work.....	18
Chapter 2. Dose verification of Drosophila (fruit fly) larva.....	19
2.1 Introduction.....	19
2.2 Material and Methods.....	19
2.2.1 Characterize the Mean Energy and Calculate the f-factor.....	19
2.2.2 Thermoluminescent Dosimeter Calibration	20
2.2.2.1 Individual TLD Calibration.....	20
2.2.2.2 General TLD Calibration.....	22
2.2.3 Setup.....	24
2.3 Results	25
2.4 Conclusion.....	27
Appendix A: RADEYE Measurements of CT Scatter and RADEYE Response Time Verification.....	28
A.1 Introduction.....	28
A.2 Materials and Methods: RADEYE Measurements of CT Scatter	28
A.2.1 Setup.....	28
A.2.2 Dose Rate Measurement.....	29
A.3 Materials and Methods: RADEYE Response Time Verification	30
A.3.1 Materials	30
A.3.2 Methods	32
A.4 Results	33
A.4.1 Accumulated Dose	33

A.4.2 Dose Rate	33
A.5 Conclusion.....	33
A.6 Future Work	34
Appendix B: RADEYE Measurements of Digital Tomography Scatter	35
B.1 Introduction	35
B.2 Materials and Methods.....	35
B.3 Results.....	37
B.4 Conclusion	37
B.5 Future Work.....	37
References	38

List of Tables

Table 1: Filter thickness derived using HVL matching	10
Table 2: DSCT Protocol.....	14
Table 3: Validation results	16
Table 4: Effective dose for male, female, average, and AAPM method	17
Table 5: Irradiation protocol.....	20
Table 6: Drosophila larvae dose rate	25
Table 7: CT Protocol.....	32
Table 8: Accumulated dose comparison.....	33
Table 9: Dose rate comparison	33

List of Figures

Figure 1: Difference between SSCT and DSCT [1]	2
Figure 2: MOSFET dosimeter energy dependence.....	3
Figure 3: SpekCalc main window.....	5
Figure 4: SpekCalc input values.....	6
Figure 5: 80kVp/Sn140kVp spectrum without tube current correction	7
Figure 6: 80kV/Sn140kV spectrum with tube current correction	7
Figure 7: 80kV and Sn140kV combined spectrum.....	8
Figure 8: f-factor variation	9
Figure 9: MOSFET calibration setup without added filtration.....	10
Figure 10: MOSFET calibration with added filtration	11
Figure 11: Film showing ion chamber and MOSFET detectors.....	11
Figure 12: 0.18cc Ion Chamber	12
Figure 13: 0.18cc ion chamber energy dependence [4]	12
Figure 14: Middle image of CTDI body phantom showing the 0.18cc ion chamber.....	13
Figure 15: MOSFET detectors.....	13
Figure 16: Middle image of CTDI body phantom showing the MOSFET detectors	14
Figure 17: Phantom setup/scanning region for abdomen/pelvis scan.....	15
Figure 18: Calibration factor per MOSFET detector.....	16
Figure 19: Organ dose distribution for Abd/Plv protocol	17
Figure 20: Drosophila Food Media Ingredients [8]	20

Figure 21: TLD's surrounding 0.18cc ion chamber	21
Figure 22: Plot of TLD sensitivity	21
Figure 23: TLD Calibration Location Setup.....	23
Figure 24: TLD general calibration	23
Figure 25: Food media phantom dimensions.....	24
Figure 26: TLD locations	25
Figure 27: Dose distribution using general calibration.....	26
Figure 28: Dose distribution using individual TLD calibration	26
Figure 29: CT room RADEYE locations	29
Figure 30: RADEYE Dosimeter	30
Figure 31: 451p Ion Chamber	31
Figure 32: Water Phantom	31
Figure 33: Dosimeter Setup.....	32
Figure 34: XR656 RADEYE locations.....	35
Figure 35: Ion chamber and RADEYE at 45 degrees.....	36
Figure 36: Ion chamber and RADEYE at 90 degrees.....	36
Figure 37: Maximum DR comparison between RADEYE and Ion Chamber.....	37

Acknowledgements

I would like to acknowledge the support of my advisor, Dr. Terry Yoshizumi, and Giao Nguyen from the Duke Radiation Dosimetry Laboratory. Without their advice and support, I would not have been able to complete this document. I would also like to thank my committee members, Dr. Robert Reiman and Dr. James Colsher, for their time and effort. I would also like to thank Juan Carlos Ramirez-Giraldo from Siemens Medical Solutions for sharing his knowledge and expertise on Siemens DSCT and Carolyn Lowry from the Department of Radiology for sharing her knowledge and expertise on Duke clinical DSCT protocols and willingness to work late hours on experiments performed at Duke Cancer Center. I would also like to acknowledge the financial support I received from Duke Radiation Dosimetry Laboratory and the United States Air Force.

I would like to thank Chu Wang, Matthew Belley, and Natalie Januzis for their help in performing the many experiments involved in this project. I would also like to thank my wife for her support and willingness to take care of our children during the long days and late nights I spent at Duke University.

Chapter 1. A Novel Approach for Effective Dose Measurements in Dual-Energy

1.1 Introduction

Dual Energy Computed Tomography (DECT) has a number of advantages over conventional Computed Tomography (CT): it has improved image registration, over conventional CT, gives material discrimination, and may reduce the dose to larger patients [1]. A concern with DECT would be the difficulty to measure organ dose with internal dosimeters due to the energy dependence. This paper will introduce a novel approach to overcome this difficulty of measuring organ dose in a dual-energy (DE) environment.

1.1.1 Dual Energy Computed Tomography vs. Conventional Computed Tomography

For this study a Dual-Source CT (DSCT) was used to produce the DE environment. The difference between conventional Single-Source CT (SSCT) and DSCT is SSCT has one x-ray source, operating at one energy level, and provides one set of images, while a DSCT has two x-ray sources, that can operate at two energy levels, and acquires two sets of images within milliseconds of each other [1]. This difference is shown in figure 1.

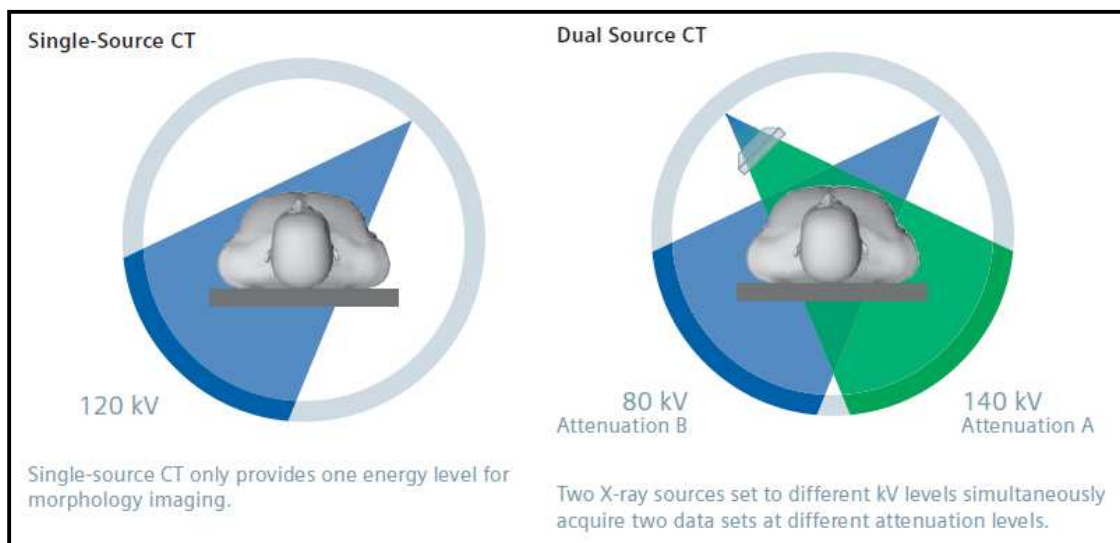


Figure 1: Difference between SSCT and DSCT [1]

1.1.2 Advantages of DSCT

Two advantages of DSCT are; more precise image registration and improved material discrimination [1]. Due to the rotation speed of the DSCT each image is taken within milliseconds of each other. This speed reduces motion artifacts which allows the image registration to be more precise. DSCT utilizes two different energy spectra which

can provide improved material discrimination due to differences in attenuation. This discrimination is further improved with added filtration on the higher energy beam [2].

1.1.3 Difficulties

The best way to measure organ dose is to separate the x-ray sources and calibrate the dosimeters separately, but this is not currently possible with DSCT software since added filtration can only be applied with DE protocols. Also, many dosimeters, such as: TLD, MOSFET, etc. are energy dependent as shown by figure 2.

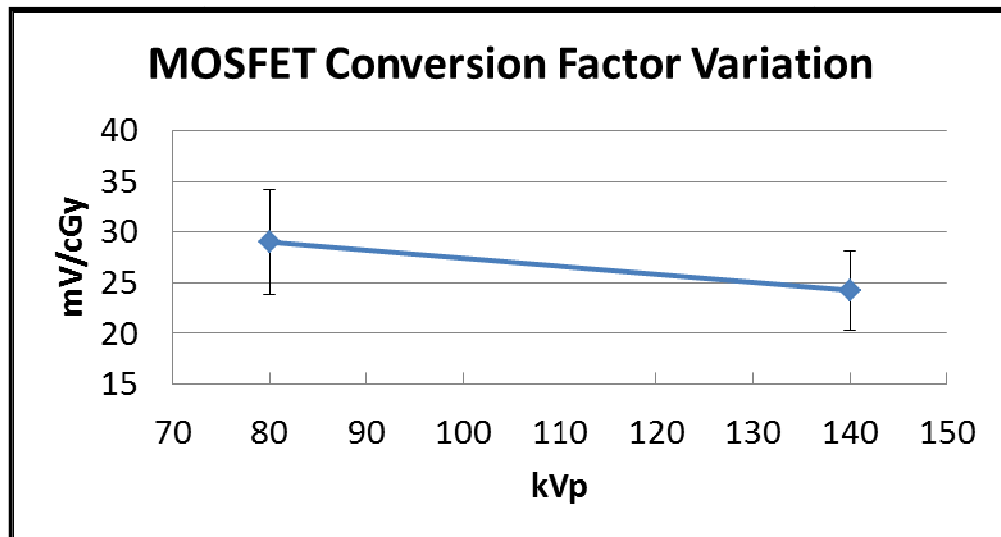


Figure 2: MOSFET dosimeter energy dependence

Other dosimeters such as an ion chamber are too large to be placed within the phantom for dose measurements.

1.1.4 Objective

Our goal was to test a novel concept approximating organ dose measurements using the single mean energy of the combined energy spectra in a DE environment.

Therefore, the purpose of this study was two-fold: (1) To obtain experimental validation of dose equivalency between MOSFET and ion chamber (as gold standard) under a dual-energy environment; (2) To estimate the effective dose (ED) using MOSFET detectors and an anthropomorphic phantom in DECT scans.

1.2 Materials and Methods

A Siemens SOMATOM Definition Flash DSCT was employed for the study. The scanner was operated at 80kVp/140kVp using an abdomen/pelvis scanning protocol. With this protocol a tin (Sn) filter is used with the higher energy x-ray tube to further separate the energy spectra. A five-phase approach was used with specific goals for each phase as follows: (1) Characterize the mean energy from the combined clinical 80kVp/140kVp beams taking into account the added Sn filtration; (2) Estimate the f -factor for soft tissue from the mean energy; (3) Calibrate the MOSFET detectors using the mean energy; (4) Validate MOSFET calibration; (5) Measure organ dose for a typical abdomen/pelvis scan using a male anthropomorphic phantom and derive ED using ICRP 103 tissue weighting factors.

1.2.1 Characterize the mean energy from the combined clinical 80kVp/140kVp (Sn added) beams

In order to characterize the mean energy of the combined 80kV/Sn140kV beams each individual spectrum for 80kV and 140kV was approximated using SpekCalc spectrum analyzing software [5]. This was done by adding filtration to the individual energy spectra to match the HVL found in the SOMATOM Definition Flash System Owner Manual [9].

The main window of SpekCalc contains three areas: an area for user defined variables such as peak energy and filter thickness, a window to output the energy spectrum, and an area to output values for HVL, Mean energy, etc.

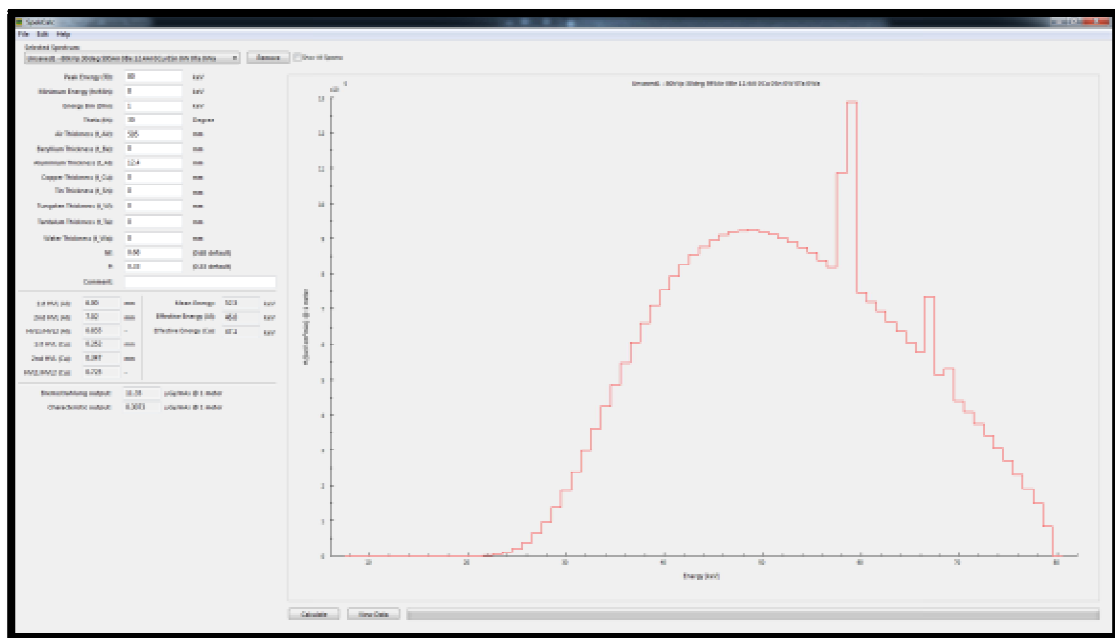


Figure 3: SpekCalc main window

Filter thickness can be added in the top left portion of the main window and the mean energy, HVL, and spectrum will be calculated based on these input values:

Peak Energy (T0):	80	keV
Minimum Energy (hvMin):	8	keV
Energy Bin (Dhv):	1	keV
Theta (th):	30	Degree
Air Thickness (t_Air):	595	mm
Beryllium Thickness (t_Be):	0	mm
Aluminium Thickness (t_Al):	12.4	mm
Copper Thickness (t_Cu):	0	mm
Tin Thickness (t_Sn):	0	mm
Tungsten Thickness (t_W):	0	mm
Tantalum Thickness (t-Ta):	0	mm
Water Thickness (t_Wa):	0	mm
Nf:	0.68	(0.68 default)
P:	0.33	(0.33 default)
Comment:		

Figure 4: SpekCalc input values

By varying the thicknesses of aluminum, the HVL for the 80kV and Sn140kV spectrum was matched with the HVL found in the DSCT technical manual and the spectrum for each beam was approximated and exported to Excel™ spreadsheet software (Microsoft Corp., Redmond, WA):

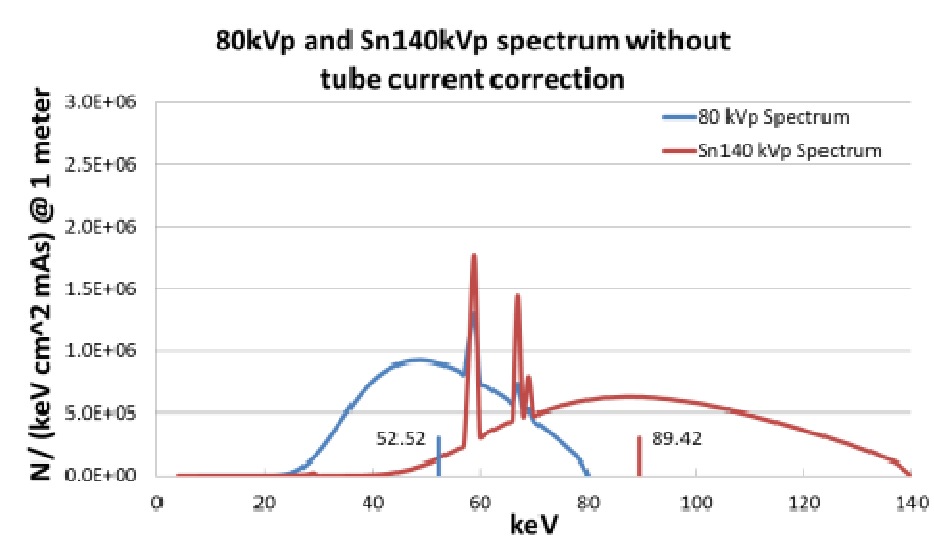


Figure 5: 80kVp/Sn140kVp spectrum without tube current correction

While operating under clinical DSCT protocols the current on the 80kVp side is boosted by a ratio of approximately 2:1 to compensate for the greater attenuation of the 80kVp beam. Since tube current is directly proportional to the number of spectra emitted, the number of spectra for the 80kV beam calculated by SpekCalc was doubled:

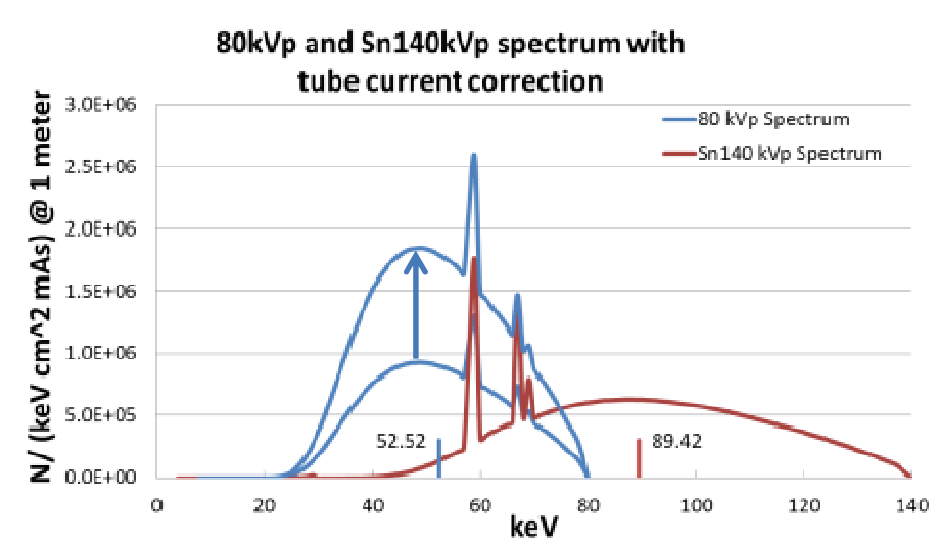


Figure 6: 80kV/Sn140kV spectrum with tube current correction

The spectra were then combined:

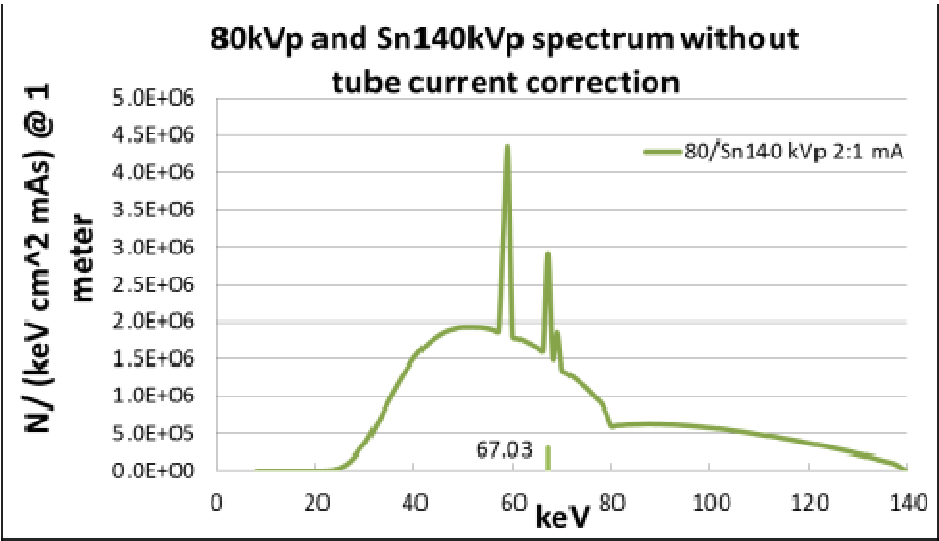


Figure 7: 80kV and Sn140kV combined spectrum

And the mean energy was found using:

$$\text{---} \quad (1)$$

1.2.2 Estimate the f-factor

To calibrate the MOSFET detectors an f-factor was used to convert an in air dose to that of another medium, in this case tissue. It was calculated by using:

$$\frac{\text{---}}{\text{---}} \quad (2)$$

Where --- represents the mass attenuation absorption coefficient for the medium being irradiated, in this case tissue, and --- represents the mass attenuation absorption coefficient of air.

Typically the mean energy of the CT beam is used to calculate the f-factor, since there are two beams in DSCT the mean energy of the combined spectrum was used due to minimal variation in the f-factor between the mean energy of the separate beams.

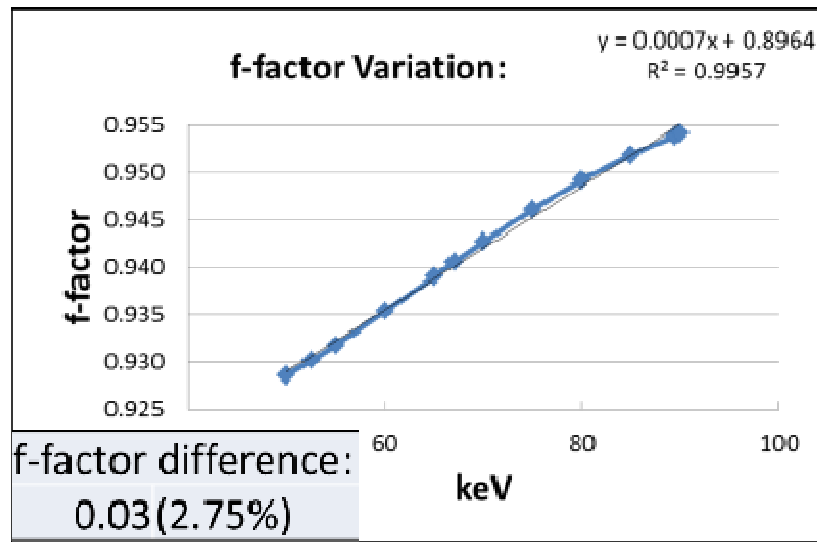


Figure 8: f-factor variation

1.2.3 MOSFET Detector Calibration:

A GE 750HD-Discovery CT (General Electric Company, Fairfield, CT) operating at 120 kVp was used to calibrate the MOSFET detectors. HVL matching in SpekCalc was used to correlate the GE beam with the DSCT combined beam. Filters were then applied until the HVL measured by a Piranha™ multifunction x-ray meter (RTI Electronics, Mölndal, Sweden) matched the HVL found using SpekCalc software:

Table 1: Filter thickness derived using HVL matching

GE 750HD-Discovery (120kVp):		
HVL SpekCalc:	8.95	mm Al
120kVp mean energy:	67.0	keV
HVL Piranha:	8.91	mm Al
Filters:	2mm Al, 0.1mm Cu	

During calibration, Gafchromic® film (Ashland Corp., Wayne, NJ) was placed under the 6cc ion chamber (Radcal Corp. Monrovia, CA) and MOSFET detectors to ensure that they were both within the beam and under the filtration:

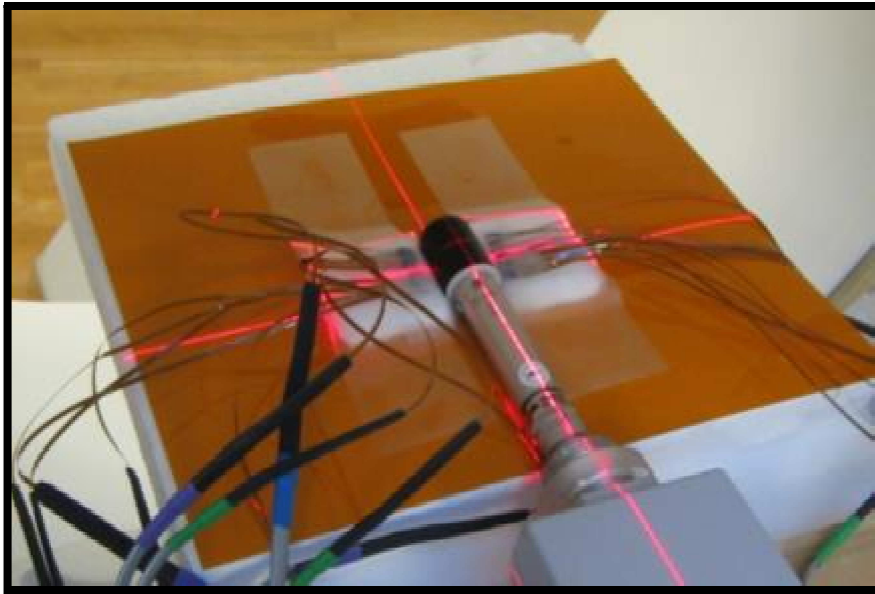


Figure 9: MOSFET calibration setup without added filtration

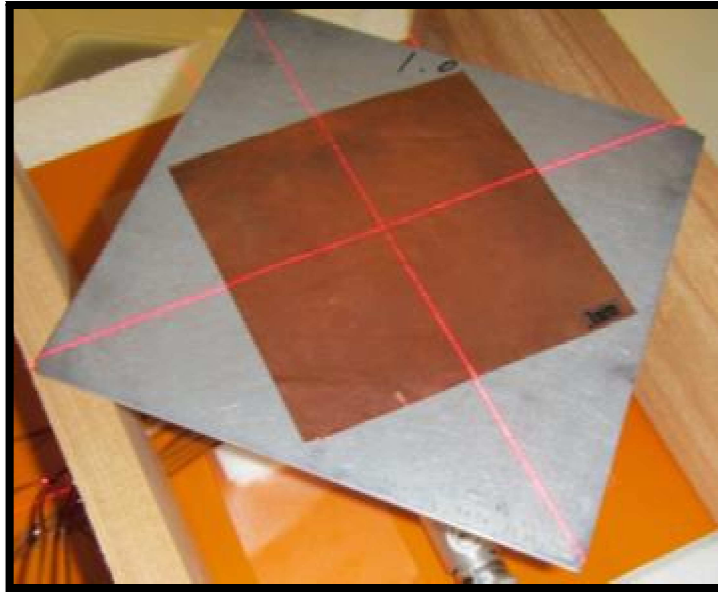


Figure 10: MOSFET calibration with added filtration

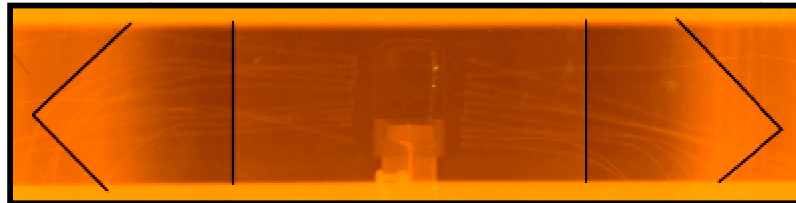


Figure 11: Film showing ion chamber and MOSFET detectors

The calibration factor for each MOSFET could then be found using:

$$\text{Calibration Factor} = \frac{\text{Ion Chamber Reading}}{\text{MOSFET Reading}} \quad (3)$$

1.2.4 Calibration validation

To validate the calibration of the MOSFET detectors a 0.18cc ion chamber (Radcal Corp. Monrovia, CA) was chosen due to its size and relative energy independence within the range of 40-140 keV [4] as shown by figure 13:



Figure 12: 0.18cc Ion Chamber

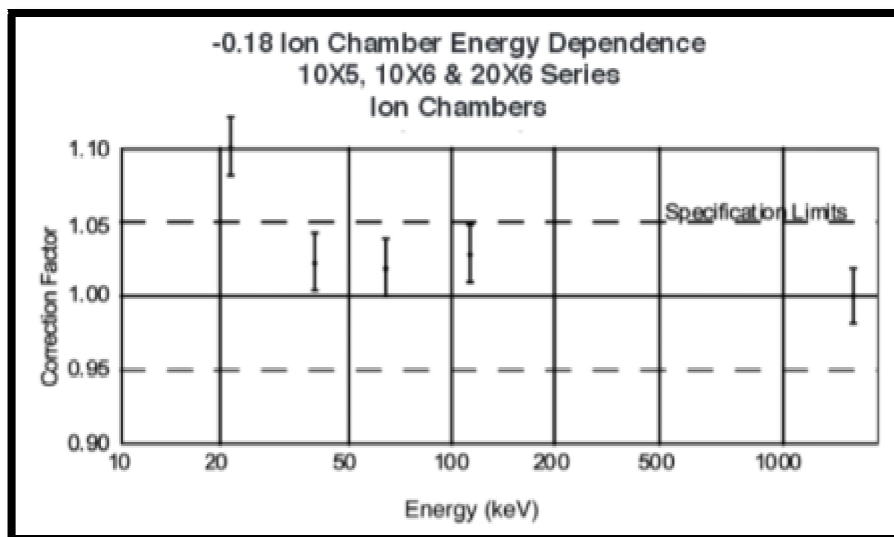


Figure 13: 0.18cc ion chamber energy dependence [4]

The ion chamber was placed in the center of a CTDI body phantom (West Physics, Atlanta, GA) and irradiated to match an abdomen/pelvis protocol.

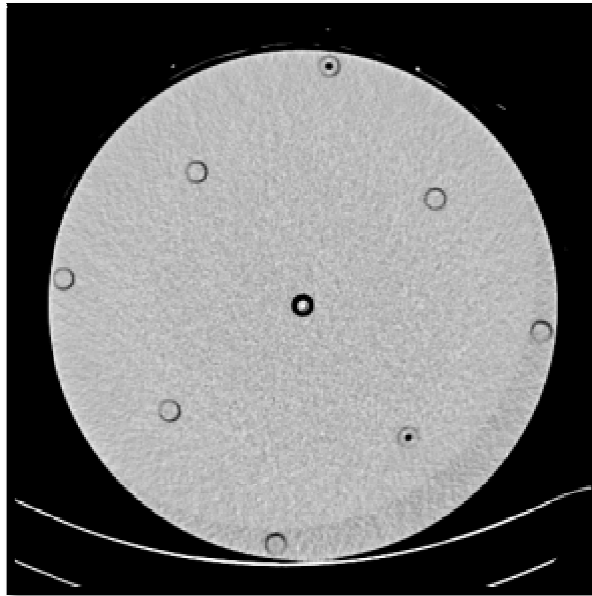


Figure 14: Middle image of CTDI body phantom showing the 0.18cc ion chamber

The ion chamber was then replaced with two MOSFET detectors and the scanning protocol was repeated.



Figure 15: MOSFET detectors

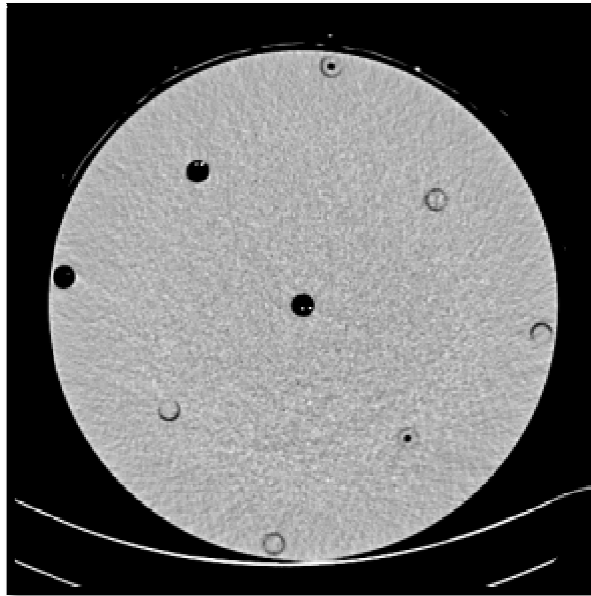


Figure 16: Middle image of CTDI body phantom showing the MOSFET detectors

1.2.5 Organ Dose Measurement with DSCT

MOSFET detectors were placed within an adult anthropomorphic phantom (Computerized Imaging Reference Systems Inc., Norfolk, VA) corresponding to organs within the abdomen/pelvis region. The phantom was then irradiated using the following protocol:

Table 2: DSCT Protocol

Protocol:		
	Tube A:	Tube B:
Protocol:	Abd/Plv	
kVp:	80	Sn140
Eff. mAs:	208	88
CTDI vol proj:	9.38 mGy	
DLP:	370.8 mGy-cm	

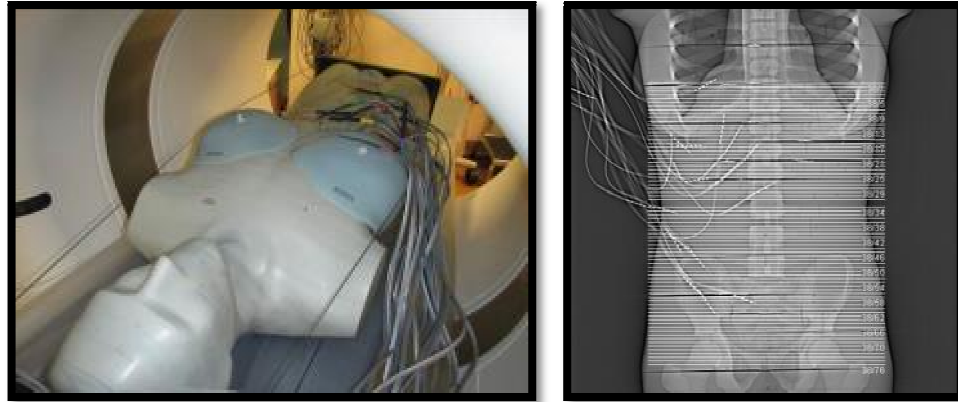


Figure 17: Phantom setup/scanning region for abdomen/pelvis scan

The standard deviation for each measurement was found using the $n-1$ method. Organ dose was corrected for percent volume scanned, skin was corrected using the “rule of nines”, bone marrow distribution was corrected using the distribution of red bone marrow in different bones of a standard man [6], and bone surface was corrected using ICRP 89 table 9.2.

1.3 Results

The mean energy of the combined DSCT spectra was calculated to be 67 keV and the f -factor for soft tissue was 0.94.

The calibration factors for the MOSFET detectors are shown in figure 18:

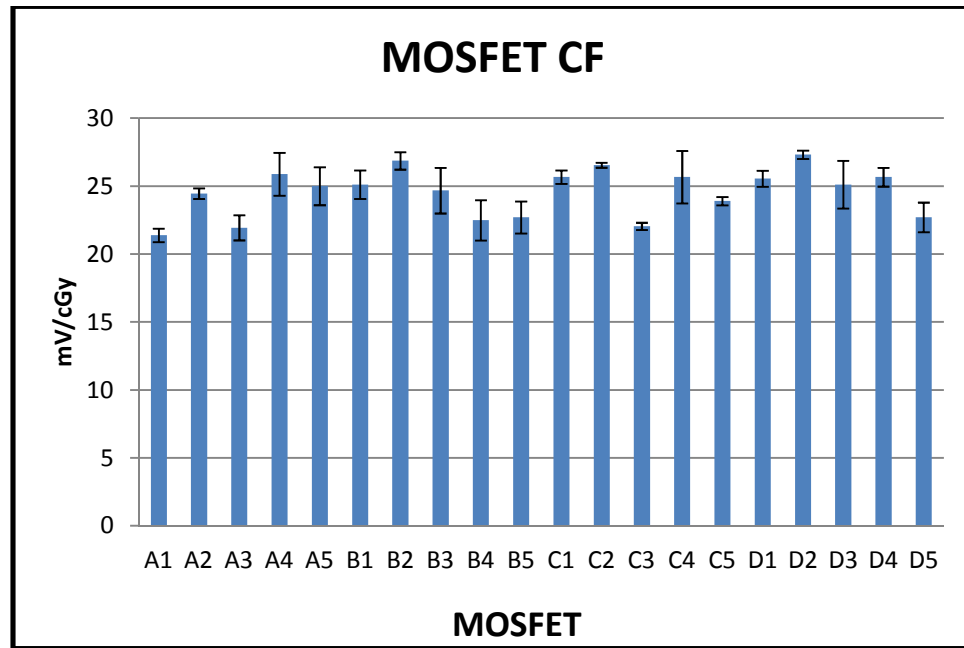


Figure 18: Calibration factor per MOSFET detector

The results from the validation are found in table 3:

Table 3: Validation results

Results(cGy):		(p = 0.15)
0.18 ion:	MOSFET:	Difference:
2.08±(2.70%)	2.20±(4.82%)	5.91%

The p value from a student's T-test was greater than 0.05 which means the difference in the measured values are not statistically significant. Also, the percent difference between the two measurements is below 10 percent. This shows that the mean energy of the combine DSCT spectrum can be used to calculate organ dose measurements.

Figure 15 shows the organ dose distribution for an abdomen/pelvis protocol:

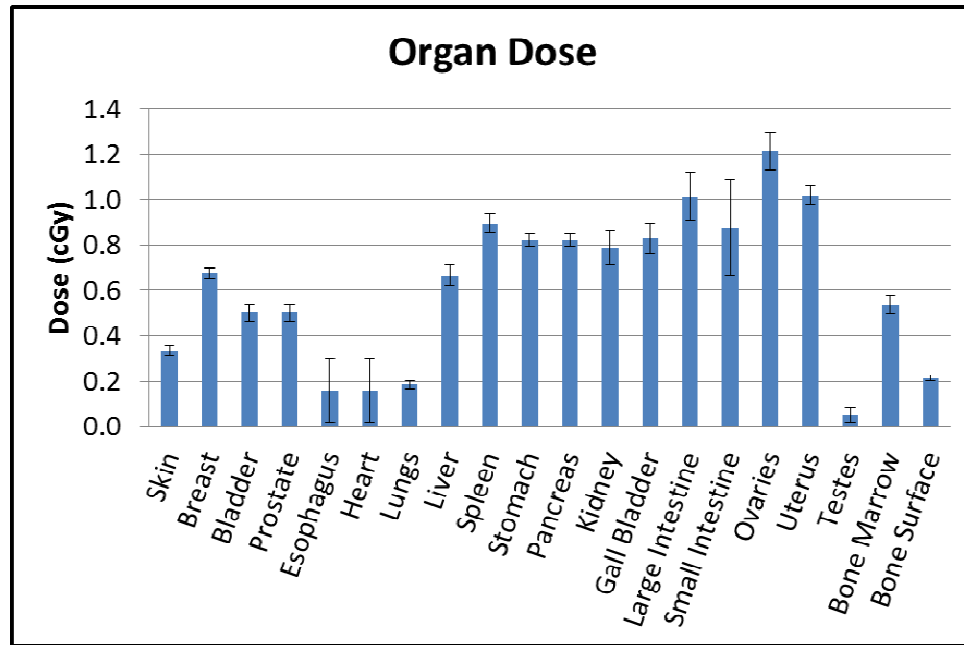


Figure 19: Organ dose distribution for Abd/Plv protocol

The effective dose from the scanning protocol discussed in section 1.2.5 for male, female, and the average of the two are given in table 2:

Table 4: Effective dose for male, female, average, and AAPM method

Effective Dose (mSv):			
Male:	Female:	Average:	AAPM:
4.12±(3.85%)	5.90±(2.93%)	5.01±(2.34%)	5.56

The AAPM value was found by multiplying the DLP from the scanning protocol by a value given in AAPM report 96.

1.4 Conclusion

This study has shown that the mean energy of the combined spectrum in DSCT can be used to measure the ED using MOSFET detectors. The ED for an adult abdomen/pelvis scan was approximately 5 mSv.

1.5 Discussion

There were two interesting observations from this study: the error from the dose measurement for the heart/esophagus was large and the Effective dose to a female was greater than the dose to a male.

The large error in the dose measurement from the heart/esophagus occurred due to the MOSFET location being outside the scanning region. This means the dose to the heart/esophagus was from scatter and resulted in a large variation in the measurement.

The number of radiosensitive organs within the scanning region for a female was greater than that of a male. This leads to a female receiving a higher dose than a male.

1.6 Future work

This method of using the mean energy in DSCT to measure the accumulated dose using MOSFET detectors could also be applied to other dual energy scenarios. The next step will be to apply this method to other dual source and dual energy CT protocols.

Chapter 2. Dose verification of *Drosophila* (fruit fly) larva

2.1 Introduction

Drosophila larvae were placed within food media and irradiated using an X-Rad 160 Biological Irradiator (X-Rad) (Precision X-Ray, North Branford, CT) to achieve a specified dose to the larvae. This was done to study the effects of radiation on the maturation of the larva. The dose to the larva was found mathematically without any physical measurements.

The purpose of this study was to establish the dose rate (DR) to the larvae within the food media for a previously used protocol using an ion chamber and thermoluminescent dosimeters (TLD's). The DR could then be used to verify that the desired dose to the *Drosophila* Larvae was achieved.

2.2 Material and Methods

2.2.1 Characterize the Mean Energy and Calculate the f-factor

The mean energy was found using SpekCalc spectrum analyzing software (5) by applying the specification for the X-Rad 160 x-ray tube (7) to calculate the mean energy.

The f-factor was then found using equation 2 with water chosen as the medium to convert the in air dose to the dose in the food media. Water was chosen due to it being the main ingredient in the food media:

<i>The recipe</i>			
	Water	2.66	liters
	Yeast	33	grams
	Yellow cornmeal	163	grams
	Agar*	16	grams
	Molasses	200	milliliters
	10% p-Hydroxy-benzoic acid methyl ester in 95% ethanol	38	milliliters

Figure 20: Drosophila Food Media Ingredients [8]

2.2.2 Thermoluminescent Dosimeter Calibration

Two methods were used to calibrate a batch of TLD's: an individual TLD calibration and a general TLD calibration. The individual TLD calibration was used to calculate the DR to the TLD's due to this method being more precise, while the general method was used to confirm the individual calibration results.

2.2.2.1 Individual TLD Calibration

For the individual TLD calibration, all of the TLD's were placed around a 0.18cc ion chamber and irradiated for 90 seconds using the following protocol:

Table 5: Irradiation protocol

X-Rad 160		
Energy:	160	kVp
Current:	18.75	mA
Filter:	F1 (2mm Al)	
Source to Target Distance:	40	cm

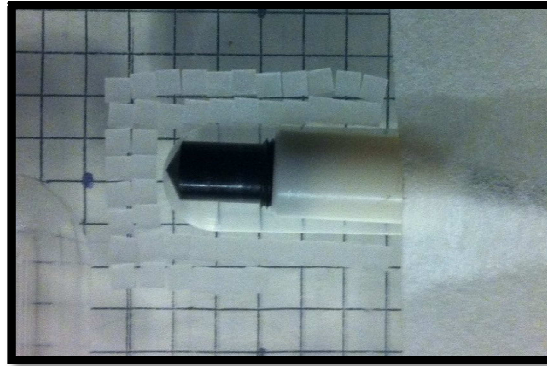


Figure 21: TLD's surrounding 0.18cc ion chamber

The reading from each TLD was then plotted to show the variation in TLD sensitivity for this protocol:

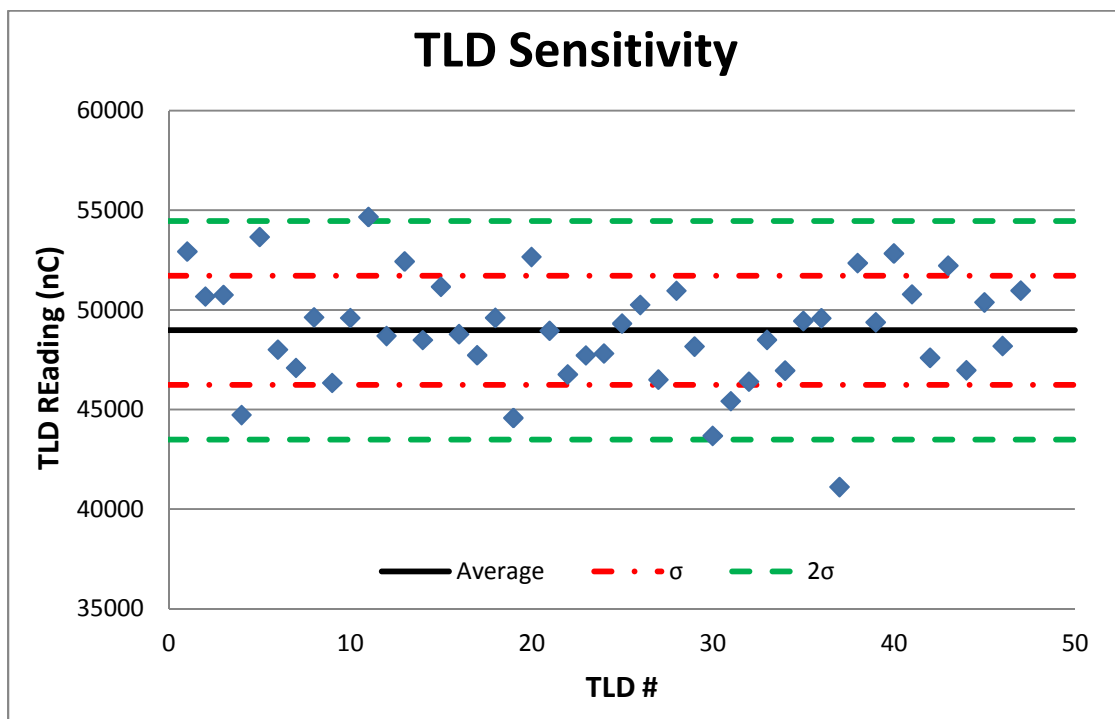


Figure 22: Plot of TLD sensitivity

As shown by the above figure each TLD reading can vary from the average by as much as three standard deviations. In order to compensate for this variation, each TLD was given its own calibration factor using the following equation:

$$\begin{aligned} & \text{TLD Calibration Factor } \left(\frac{\text{cGy}}{\text{nC}} \right) \\ &= \frac{(\text{Ion Chamber reading}) * (\text{Ion Chamber Correction Factor}) * (f - \text{factor})}{(\text{TLD reading}) - (\text{Background})} \quad (3) \end{aligned}$$

Where the Ion Chamber Reading gives an uncorrected dose in rem and the f-factor converts the in air dose (rem) to the dose in water (cGy). These calibration values could then be applied when approximating the DR to the drosophila larvae.

2.2.2.2 General TLD Calibration

For general calibration, some of the TLD's are set aside, irradiated at different time intervals, and plotted alongside the ion chamber dose for each irradiation. A polynomial fit can then be applied and the resulting equation can be used to calculate the dose to any TLD within the batch.

A 0.18cc ion chamber was used to calibrate four sets, sixteen total, of TLD's with each set being irradiated for 30, 60, 90, and 120 seconds respectively. The calibrations were done using an X-Rad 160 and the protocol described in section 2.2.2.



Figure 23: TLD Calibration Location Setup

The results were then plotted and fit to a line:

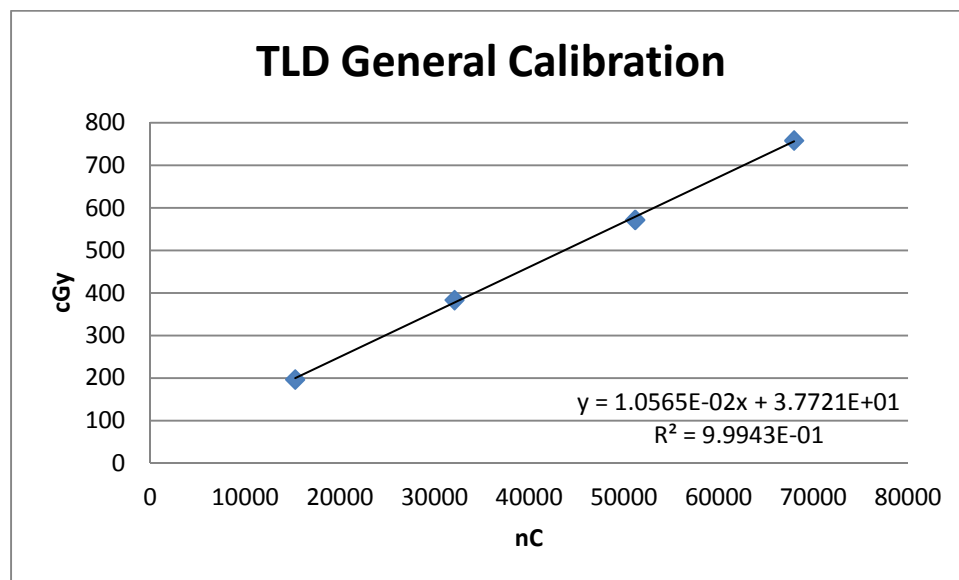


Figure 24: TLD general calibration

The resulting equation was then used to find the dose to each TLD.

2.2.3 Setup

To calculate the DR, an acrylic phantom was manufactured to duplicate the scatter associated with placing the food media in a petri dish. The phantom was made to fit inside the dish, had five TLD locations, and had the following dimensions:

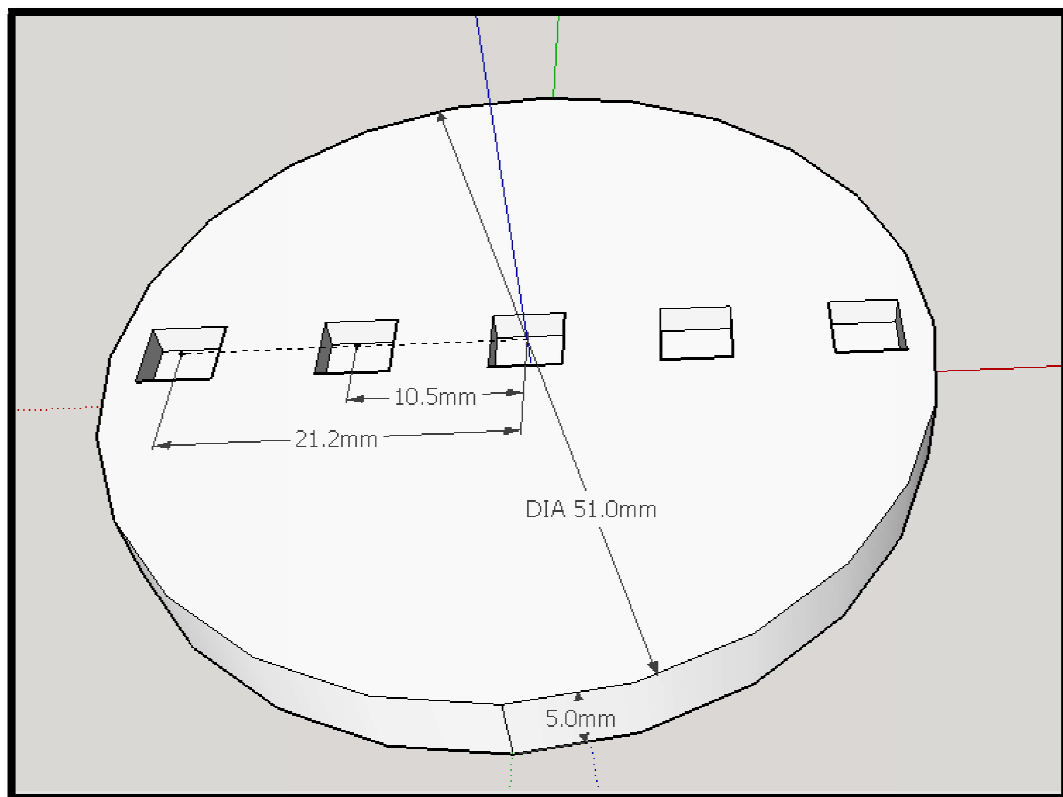


Figure 25: Food media phantom dimensions

TLD's, two per location, were then placed in the phantom:

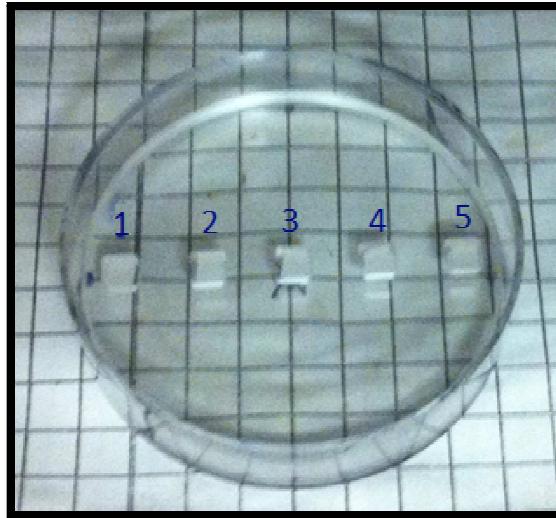


Figure 26: TLD locations

The TLD's were then irradiated for 90 seconds using the protocol described in section 2.2.2. This process was then repeated with a new set of TLD's.

Both the individual and general calibrations were then applied to the TLD's and the results compared.

2.3 Results

The mean energy was found to be 59.8 keV which gave an f-factor of 0.9156 and resulted in the following values for the general and individual TLD calibrations:

Table 6: Drosophila larvae dose rate

DR (Gen. Cal.):	5.02±(17.75%)	cGy/sec
DR (Ind. Cal.):	5.19±(6.21%)	cGy/sec

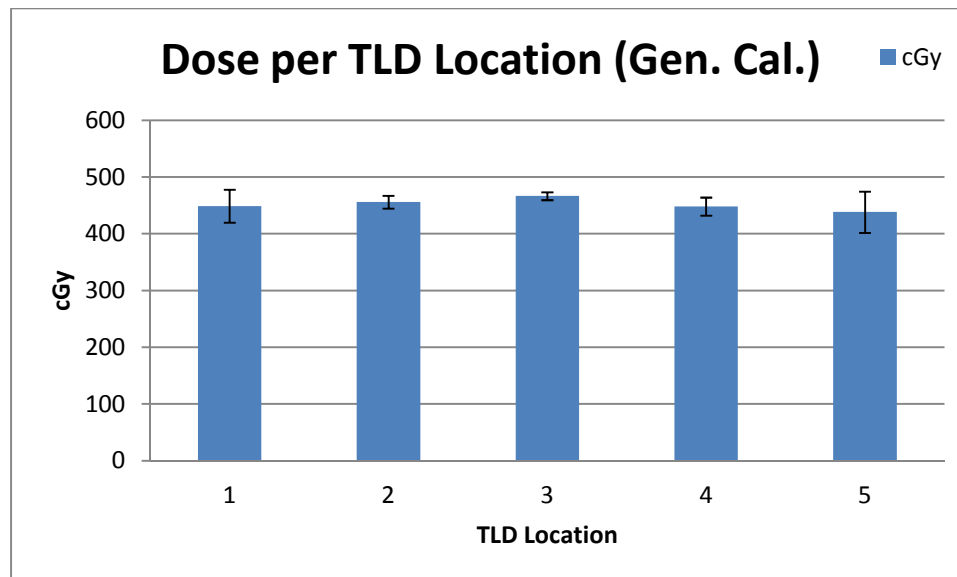


Figure 27: Dose distribution using general calibration

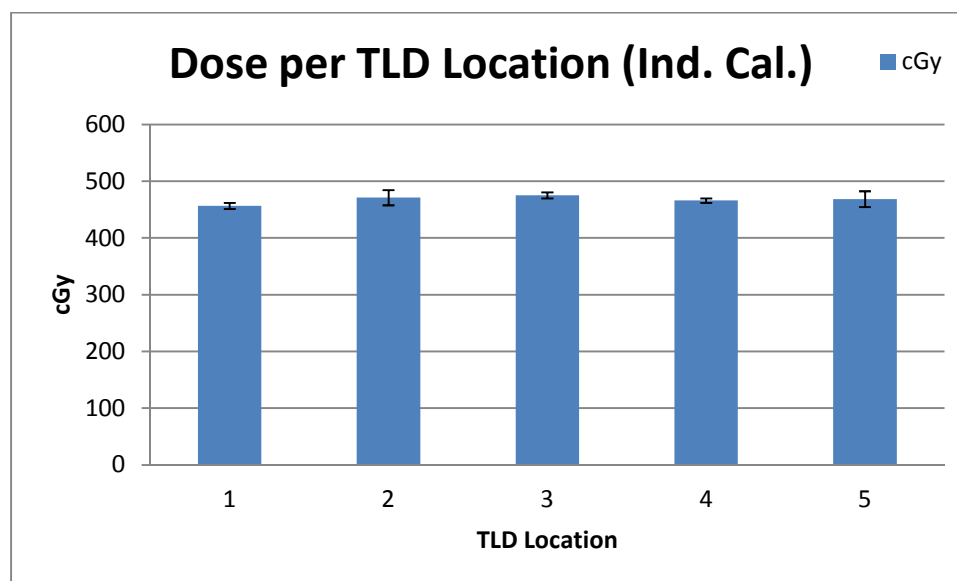


Figure 28: Dose distribution using individual TLD calibration

2.4 Conclusion

Since the individual calibration value was well within one a standard deviation of the general calibration value, this shows that the individual calibration was a good approximation to the actual DR. By using the individual TLD calibration method the error was reduced from 17.75% to 6.21%. Using this method the DR to the drosophila larvae was found to be $5.19 \pm (6.21\%)$ cGy/sec for the protocol chosen.

Appendix A: RADEYE Measurements of CT Scatter and RADEYE Response Time Verification

A.1 Introduction

The purpose of this study was to look at the accumulated dose from a CT room, apply current CT shielding, and then compare and contrast these results with what is required by ICRP 103. To measure the dose accumulated in a CT room due to scatter, we used a RADEYE™ G portable dose- and dose rate meter (RADEYE) (Thermo Fisher Scientific Inc., Erlangen, Germany.) A concurrent project, discussed in Appendix B, found that the RADEYE may not be accurate enough to measure the shorter scan times for CT's. This changed the purpose of this study to verifying the response time of the RADEYE dosimeters.

A.2 Materials and Methods: RADEYE Measurements of CT Scatter

A.2.1 Setup

In order to measure the scatter in the CT room, RADEYE dosimeters were placed in four locations:

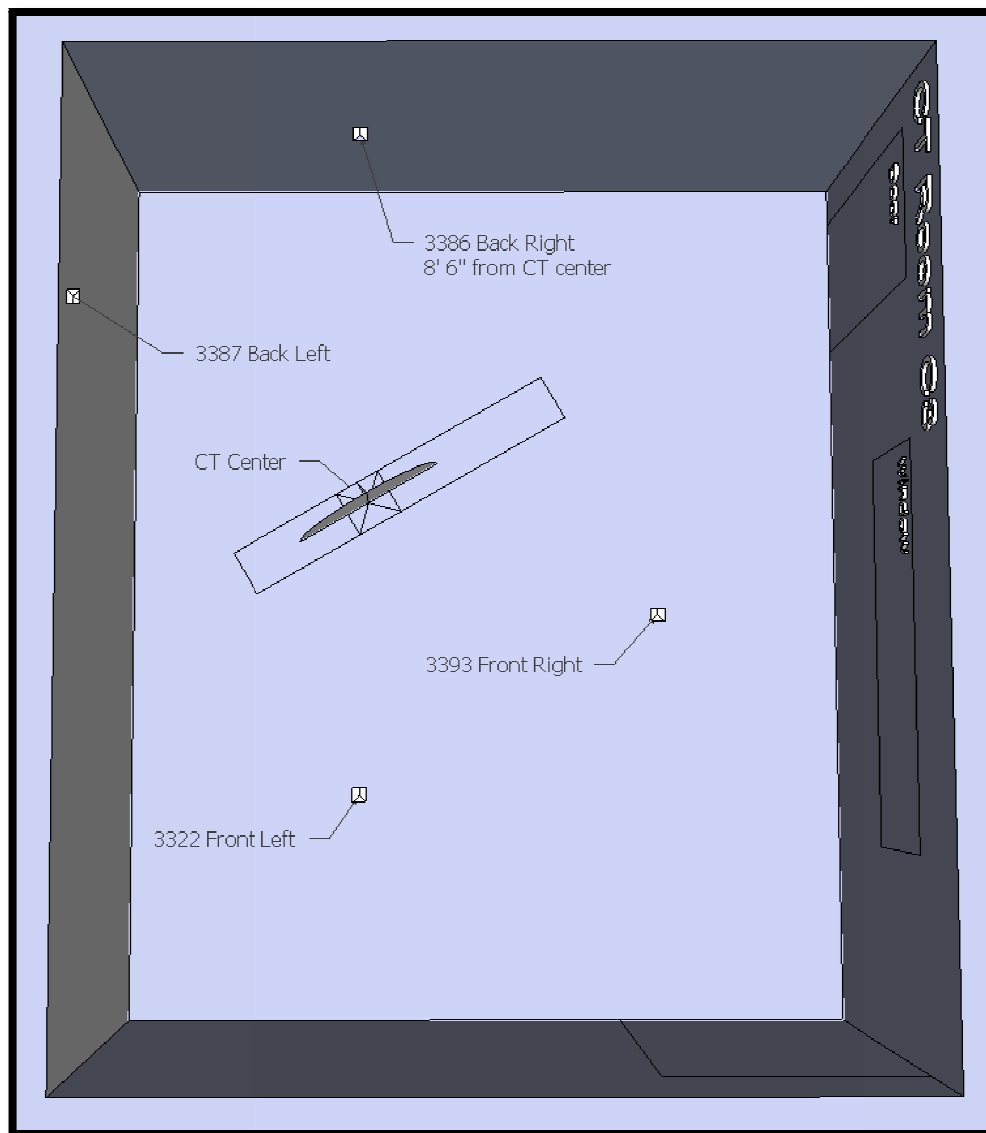


Figure 29: CT room RADEYE locations

A.2.2 Dose Rate Measurement

The DR data was then downloaded from the RADEYE dosimeters at 5pm daily for two work weeks (Monday-Friday). During this time a second project was being done using the RADEYE dosimeters that showed that they may not be accurate with short

scan times (This discovery is discussed in more detail in Appendix B). At this point the study changed to verifying the response time of the RADEYE dosimeters.

A.3 Materials and Methods: RADEYE Response Time Verification

A.3.1 Materials

Four RADEYE dosimeters were used for this study.



Figure 30: RADEYE Dosimeter

Two were set to record the mean and max DR for a 30 second time interval, the third was given a 15 second time interval, and the fourth was given a 1 second time interval. The accumulated dose was also recorded after each CT scan.

A 451P ion chamber was used as a gold standard to compare to the RADEYE measurements.



Figure 31: 451p Ion Chamber

A water phantom was used to provide consistent scatter data equivalent to tissue.

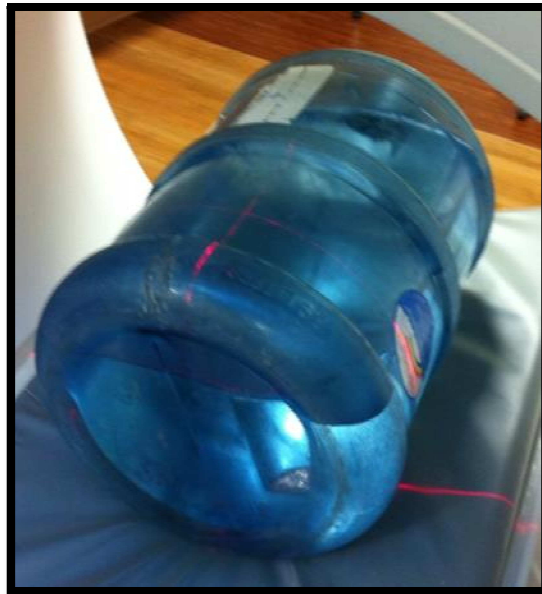


Figure 32: Water Phantom

A GE 750HD-Discovery CT was used to irradiate the water phantom.

A.3.2 Methods

The RADEYE dosimeters and the 451P were placed with the center of their ion chambers at a distance of 1 meter from the center of the CT.



Figure 33: Dosimeter Setup

The CT machine was then placed in service mode and given the following protocol:

Table 7: CT Protocol

GE 750HD-Discovery:	
CC CT2 IN62	
KVP:	120
mA:	200
time (sec):	2
Axial Scan	
runs:	2

This protocol was then run three times and the data was record after each run.

A.4 Results

A.4.1 Accumulated Dose

Table 8: Accumulated dose comparison

	Trial 1	Trial 2	Trial 3	
451P	1.87	1.87	1.65	(mR)
RADEYE	1.38±0.37	1.37±0.25	1.21±0.14	(mR)
Difference	26.06	26.65	26.66	(%)

A.4.2 Dose Rate

Table 9: Dose rate comparison

	Trial 1	Trial 2	Trial 3	
451P	1.68	1.68	1.49	(R/hr)
RADEYE	1.77±0.19	1.79±0.10	1.74±0.09	(R/hr)
Difference	5.01	6.24	16.99	(%)

A.5 Conclusion

Since the percent difference between the RADEYE measurements was about 27% for the accumulated dose and 5-17% for the max dose rate, RADEYE dosimeters can be used to measure the accumulated dose and dose rate for CT scatter.

A.6 Future Work

Due to the accumulated dose not being recorded while measuring the CT scatter data the original study will need to be repeated so the daily accumulated dose can be used to compare and contrast the requirements in the ICRP 103.

Also, further work could be done to see how the accumulated dose measurement changes with varying exposure times.

Appendix B: RADEYE Measurements of Digital Tomography Scatter

B.1 Introduction

The purpose of this study was to look at the accumulated Scatter dose from a GE Discovery XR656 Digital Radiography System (General Electric Company, Fairfield, CT), apply current room shielding, and then compare and contrast these results with what is required by ICRP 103.

B.2 Materials and Methods

RADEYE dosimeters where placed in various locations around the XR656 and the DR's were recorded daily.

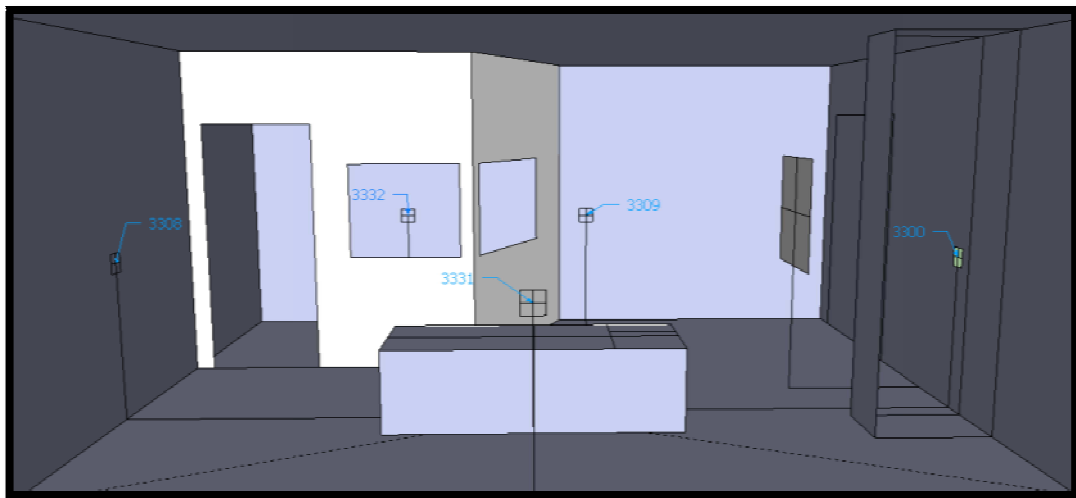


Figure 34: XR656 RADEYE locations

A one meter scatter reference was found using a 451p ion chamber and RADEYE by placing them one meter from the scatter source at 45 and 90 degree angles.



Figure 35: Ion chamber and RADEYE at 45 degrees

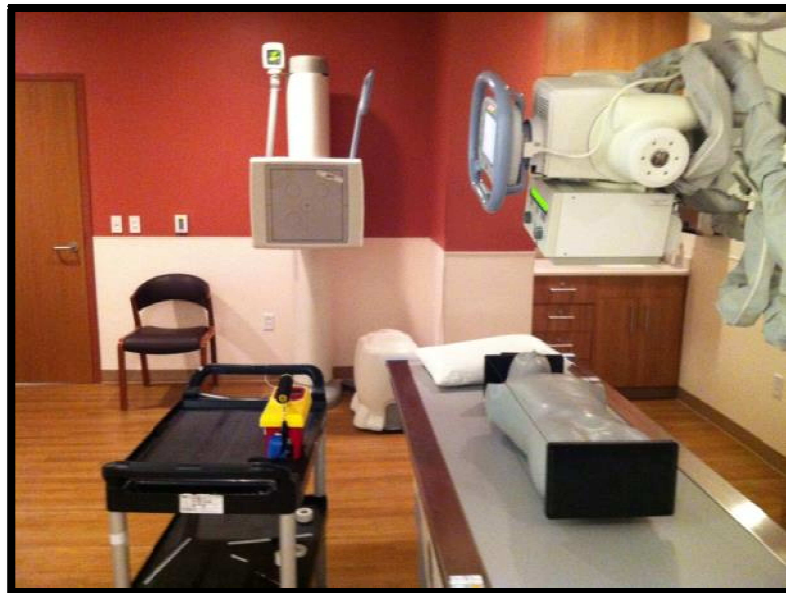


Figure 36: Ion chamber and RADEYE at 90 degrees

The maximum DR was recorded for both detectors and compared.

B.3 Results

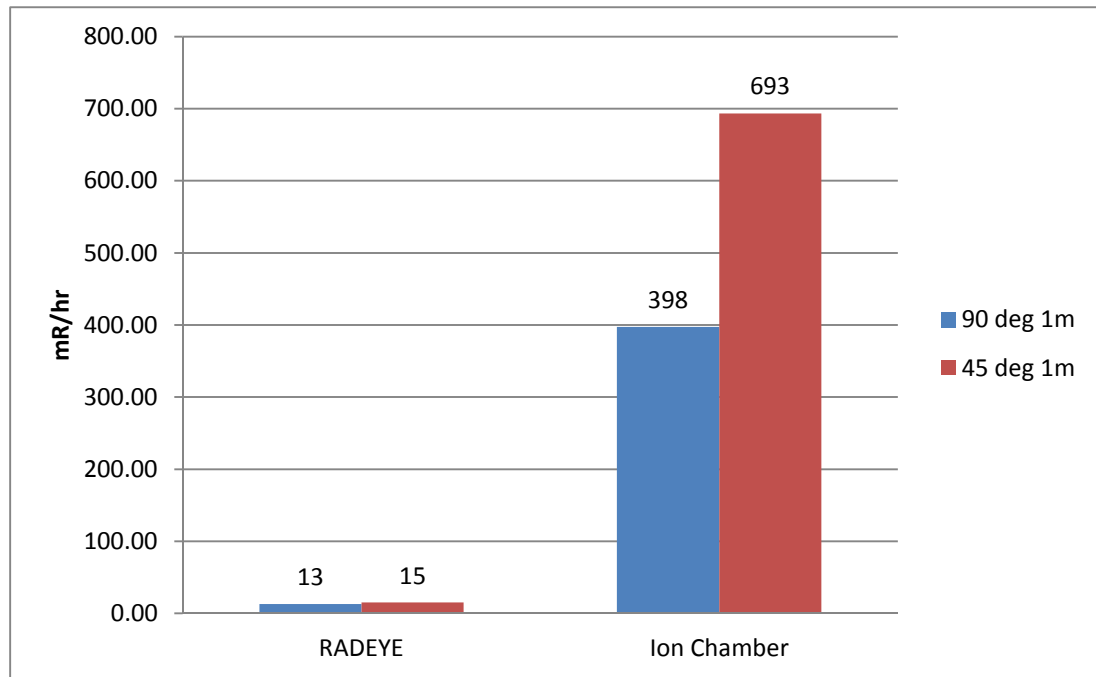


Figure 37: Maximum DR comparison between RADEYE and Ion Chamber

B.4 Conclusion

Given that the maximum DR of the RADEYE at 45 degrees was 15 mR/hr while the Ion Chamber read 693 mR/hr, the RADEYE detectors cannot be used for dose measurements with the XR656 machine. This is most likely due to the time dependence of the RADEYE dosimeters since the XR656 uses msec pulses to produce a sequence of images.

B.5 Future Work

Further testing of the RADEYE dosimeters could be done to measure their time dependence specifically for pulsed imaging.

References

1. SEIMENS. *Flash Speed. Lowest Dose. SOMATOM Definition Flash* [Brochure]. Forchhelm, Germany: N.P., 2010.
2. Primak, A. N., et al. *Improved dual-energy material discrimination for dual-source CT by means of additional spectral filtration*. Rochester, Minnesota: Am. Assoc. Phys. Med. 2009.
3. AAPM Task Group 23. *The Measurement, Reporting, and Management of Radiation Dose in CT*. College Park, MD: Am. Assoc. Phys. Med. 2008.
4. RADCAL. *Ion Chamber –Energy Dependence Graphs*. Monrovia, CA: www.radcal.com 2012.
5. Poludniowski, Gavin. G. *SpekCalc GUI*. (1.1). [Computer Program]. <http://spekcalc.weebly.com/> (n.d.)
6. Cristy M. *Active bone marrow distribution as a function of age in humans*. Phys Med Biol 1981; 26:389–400.
7. PXi Precision X-Ray. *X-RAD 160 X-Ray Biological Irradiator* [Brochure]. North Branford, CT: N.P., (n.d.)
8. Bloomington Drosophila Stock Center. *Cornmeal, Molasses and Yeast Medium*. Indiana University, IN: [http://flystocks.bio.indiana.edu/Fly Work/media-recipes/molassesfood.htm#recipe](http://flystocks.bio.indiana.edu/Fly_Work/media-recipes/molassesfood.htm#recipe) 2012.
9. SEIMENS, *System Owner Manual*, Forchhelm, Germany: N.P., (n.d.)